

# Supplementary Information for

## Extreme tunability in aluminum doped Zinc Oxide plasmonic materials for near-infrared applications

A.K. Pradhan\*, R.M. Mundle, Kevin Santiago, J.R. Skuza, Bo Xiao, K. Song, M. Bahoura, Ramez Cheaito and Patrick E. Hopkins

\* Correspondence and requests for materials should be addressed to A.K.P. (apradhan@nsu.edu)

### Materials and Methods

#### Fabrication of Al doped ZnO

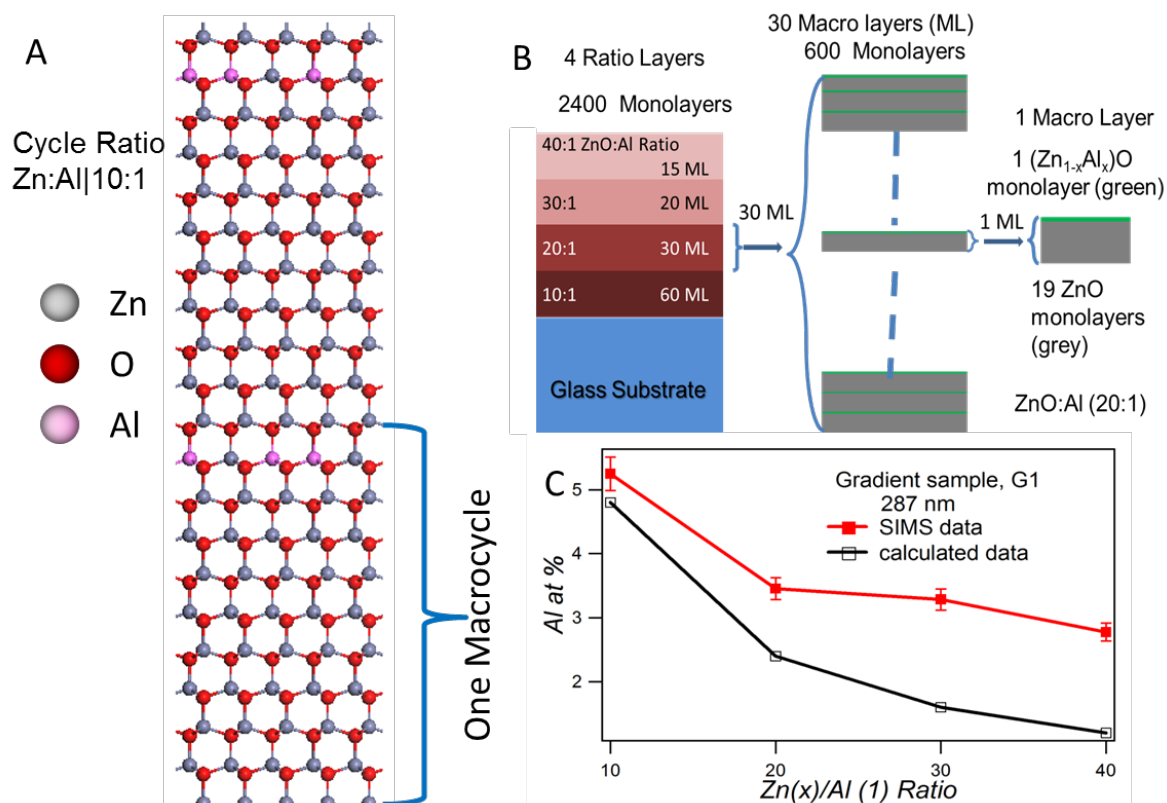


**Fig. 1 (a)** Schematics of the AZO films (Zn:Al ratio of 10:1) grown by alternating between 15 ms pulses of diethylzinc (DEZ,  $\text{Zn}(\text{C}_2\text{H}_5)_2$ ) and  $\text{H}_2\text{O}$ ; periodic 15 ms pulses of Trimethylaluminum (TMA),  $\text{Al}(\text{CH}_3)_3$ ) as the aluminum dopant with a ratio of Zn:Al=10:1 in each macrocycle. **(b)** Schematics of the G1 gradient films of AZO grown by the ALD technique.

The gradient films comprising of four Zn:Al ratios from 10:1, 20:1, 30:1 and 40:1, were fabricated as shown for each ratio. (c) The time of flight secondary ion mass spectroscopy (TOF-SIMS) of the atomic percentage of Al in each layer of the G1 gradient film is plotted versus the Zn:Al cycle ratio from 10:1, 20:1, 30:1, and 40:1.

### **Variable Angle Spectroscopic Ellipsometry (VASE)**

Variable angle spectroscopic ellipsometry (VASE) is a popular measurement technique that is used to study the optical properties of thin films. Light is directed to a sample at multiple angles and is either absorbed, transmitted or reflected. The reflected light is analyzed for intensity and polarization and from that many film properties can be determined such as film thickness, index of refraction, permittivity, absorption, etc.<sup>1,2</sup>. VASE was employed in this study to investigate some of the optical properties of the AZO films. The ellipsometer used was the HS-190 by the J.A. Woollam Company<sup>38</sup>. The probe wavelengths ranged from 1500 nm to 2500 nm in increments of 10 nm, and the scan angles were 65°, 70°, and 75°, resulting in over 300 data points per sample to model and calculate thicknesses and optical constants. The high accuracy autoretarder was employed during the measurements because of reduced beam intensity due to film transparency. The auto-retarder optimizes the light beam polarization prior to reaching the sample, producing the best measurement conditions for each sample.

Ellipsometry is an optical measurement technique that can describe light reflection characteristics from many types of thin films; from this many film parameters can be determined such as thickness and index of refraction<sup>3,4</sup>. The most important analysis parameters in ellipsometry are change in light polarization upon reflection from the sample, and phase shift of the light due to the interaction with the sample. These two parameters are  $\Psi$ , and  $\Delta$ , respectively. They are related through the equation (1):

$$\rho \equiv \tan(\Psi) \exp(i\Delta) \equiv \frac{r_p}{r_s} \equiv \frac{\frac{E_{rp}}{E_{ip}}}{\frac{E_{rs}}{E_{is}}} \quad (1)$$

Where  $r_p$  and  $r_s$  are the Fresnel reflection coefficients in the P and S-planes respectively, and  $\frac{E_{rp}}{E_{ip}}$  and  $\frac{E_{rs}}{E_{is}}$  are the ratios of the amplitudes of the electric fields in both P and S-planes, respectively<sup>39</sup>. From  $\Psi$  and  $\Delta$ , optical models are developed to describe the sample using the ellipsometry analysis software WVASE 32.

## Electrical measurements

Electronic transport properties were measured using a Keithley 6220 current source and a 2182A nanovoltmeter in a linear four-point probe configuration. Electrical transport measurements of low temperature resistance vs. temperature were done in an optical cryostat with a measurement range from 20 K up to 320 K. Hall Effect measurements were performed in a Quantum Design MPMS XL with a magnetic field up to 2 to 4 Tesla.

### Electrical Resistance of Al:ZnO=1:20

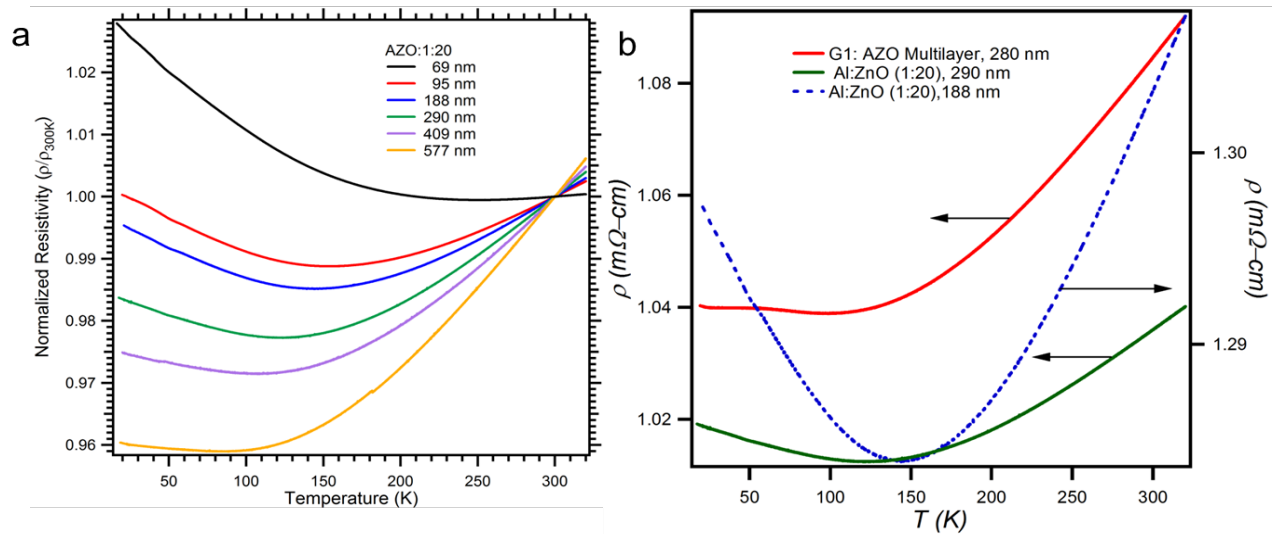


**Fig. 2 (a)** Temperature dependence of the resistance normalized to 300 K for five different AZO films (Zn:Al=20:1) with varying thickness, **(b)** Electrical resistivity ( $\rho$ ) for three various samples, including the gradient, G1 sample.

There is a large change in the resistivity going from as high as  $1.19 \times 10^{-3} \Omega\text{-cm}$  for the 69 nm film down to as low as  $7.9 \times 10^{-4} \Omega\text{-cm}$  for the 577 nm film (not shown here). The metallic behavior is due to Al donor electrons filling up the lower levels in the conduction band. This is known as the Burstein-Moss effect- as seen in degenerate semiconductors due to the impurity band of the Al donor overlapping with the ZnO conduction band. The AZO films of 290 nm thick behave more like metals. The films grown with less than 188 nm thickness show a metal to semiconductor transition. The resistivity increases with decreasing temperature due to recombination of donor electrons with Al for semiconductors. The metallic behavior comes due to the Fermi energy level shifting further above the CB, increasing the energy required by the electrons to be promoted from the impurity donor to the CB. The decrease in resistivity with decreasing temperature is due to reduction in thermal energy lowering the number of electrons vibrating with the energy needed to scatter the conducting electron, which is common in metals.

### **Thermal measurements**

We measure the thermal conductivity by time-domain thermoreflectance (TDTR)<sup>5,6</sup>. A schematic of the main components in our experiment is shown in Fig. S4. TDTR is a nondestructive optical pump-probe technique in which an 80 MHz pulse train emanates from a Ti-Sapphire laser with pulse widths of about 150 fs and wavelength of 800 nm. The laser output is split into two separate paths, a pump and probe. In our setup, the pump beam is modulated by an electro-optic modulator (EOM) driven by a function generator that supplies a sine wave modulation at 8.8 MHz frequency. The pump is focused on the sample by an objective lens. This modulation

creates an oscillatory temperature rise on the sample surface and a thermal wave that propagates through the sample at the same frequency. The probe is directed down a mechanical delay stage, focused on the sample coaxially with the pump beam, and then retroreflected into a photodetector connected to a lock-in amplifier. The lock-in amplifier extracts the components of the thermal wave at the modulation frequency. We monitor the ratio of the in-phase to out-of-phase component of the lock-amplifier response as a function of time delay between pump and probe up to time delays of about 6 ns. We assume literature values for the heat capacities of the Al film and the heat capacity and thermal conductivity of the glass substrate. We measure the electrical resistivity of the aluminum film by four-point probe and deduce the thermal conductivity from Weidman-Franz law. We set the interface conductance between the ZnO film and the glass substrate to infinity, although we are not sensitive at all to this parameter given the thickness of the ZnO film and the high modulation frequency used in our experiment. Hence the only unknowns in our thermal model are the Al/ZnO Kapitza conductance and the thermal conductivity of the ZnO film. These parameters are treated as free parameters and are varied to fit the data to a multilayer thermal model that has been detailed elsewhere<sup>5-9</sup>. Figure S4 shows the data and best fit curves for the two measured samples. The sample temperature was controlled via an cryostat with optical access. All measurements performed in the cryostat were kept under vacuum at pressures less than  $10^{-5}$  Torr.

We have taken data at higher temperatures. The thermal conductivity for the two samples is given in the table below. The thermal conductivities are relatively constant with temperature in this range.

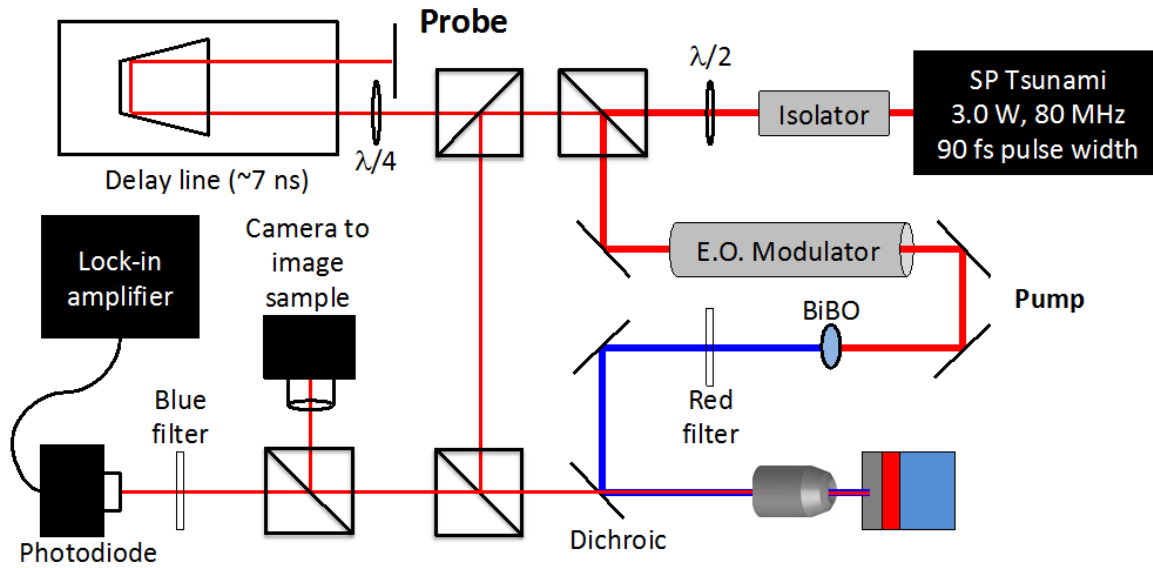


Fig. 3 A schematic of the main components of the TDTR setup used (E.O. = electro-optic).

Table 1.

T	287 nm sample		290 nm sample	
	k (W/m/K)	error (W/m/K)	k (W/m/K)	error (W/m/K)
296 K	5.65979494	0.380446438	4.260894719	0.114791988
334 K	4.743296442	0.278278978	4.200835295	0.271719847
373 K	5.435252627	0.440951165	4.272679413	0.167460929

## References

1. Woollam, J. A., Johs, B., Herzinger, C. M., Hilfiker, J., Synowicki, R. & Bungay, C. L. Overview of variable angle spectroscopic ellipsometry (VASE), part I: basic theory and typical applications. *Proc. SPIE CR72*, 3-28 (1999).
2. J.A. Woollam. Co., Vertical VASE, 2007.
3. Pascu, R. & Dinescu, M. Spectroscopic Ellipsometry. *Romanian Reports in Phys.* **64**, 135-142 (2010).

4. Tseng, A. A., Chen, K., Chen, C.D. & Ma, K. J. Electron beam lithography in nanoscale fabrication: recent development. *Electr. Pack. Manufac. IEEE Transact.* **26**, 141-149 (2003).
5. Cahill D. G., Goodson K. & Majumdar A. Thermometry and thermal transport in micro/nanoscale solid-state devices and structures. *Journal of Heat Transfer* **124**, 223 (2002).
6. Hopkins, P. E., Serrano, J. R., Phinney, L. M., Kearney, S. P., Grasser, T. W. & Harris, C. T. Criteria for cross-plane dominated thermal transport in multilayer thin film systems during modulated laser heating. *J. Heat Transfer* **132**, 081302 (2010).
7. Cahill, D. G. Analysis of heat flow in layered structures for time-domain thermoreflectance. *Rev. Sci. Instrum.* **75**, 5119 (2004).
8. Schmidt, A. J., Chen, X. & Chen G. Pulse accumulation, radial heat conduction, and anisotropic thermal conductivity in pump-probe transient thermoreflectance. *Rev. Sci. Instrum.* **79**, 114902 (2008).
9. Hopkins, P. E., Serrano, J. R., Phinney, L. M., Kearney, S. P., Grasser, T. W. & Harris, C. T. Criteria for cross-plane dominated thermal transport in multilayer thin film systems during modulated laser heating. *J. Heat Transfer* **132**, 081302 (2010).